Available online at www.sciencedirect.com
ScienceDirect
Advances in Space Research 43 (2009) 1479–1483
ADVANCES IN SPACE RESEARCH (a COSPAR publication)
www.elsevier.com/locate/asr

Coronal fast wave trains of the decimetric type IV radio event observed during the decay phase of the June 6, 2000 flare

H. Mészárosová [a,*], H.S. Sawant [b], J.R. Cecatto [b], J. Rybák [c], M. Karlický [a], F.C.R. Fernandes [d], M.C. de Andrade [b], K. Jiřička [a]

[a] Astronomical Institute, Czech Academy of Sciences, CZ-25165 Ondřejov, Czech Republic
[b] National Space Research Institute (INPE), Ave. dos Astronautas 1758, 1221-0000 São José dos Campos, SP, Brazil
[c] Astronomical Institute, Slovak Academy of Sciences, SK-05960 Tatranská Lomnica, Slovak Republic
[d] Institute of Research and Development (IP&D – UNIVAP), Ave. Shishima Hifum 2911, Urbanova, 12244-000 São José dos Campos, SP, Brazil

Received 27 October 2008; received in revised form 23 January 2009; accepted 27 January 2009

Abstract

The 22 min long decimetric type IV radio event observed during the decay phase of the June 6, 2000 flare simultaneously by the Brazilian Solar Spectroscope (BSS) and the Ondřejov radiospectrograph in frequency range 1200–4500 MHz has been analyzed. We have found that the characteristic periods of about 60 s belong to the long-period spectral component of the fast wave trains with a tadpole pattern in their wavelet power spectra. We have detected these trains in the whole frequency range 1200–4500 MHz. The behavior of individual wave trains at lower frequencies is different from that at higher frequencies. These individual wave trains have some common as well as different properties. In this paper, we focus on two examples of wave trains in a loop segment and the main statistical parameters in their wavelet power and global spectra are studied and discussed.

Keywords: Sun; Corona; Flares; Radio radiation; MHD waves

1. Introduction

It has been theoretically predicted (Roberts et al., 1983, 1984) that periodicity of fast magnetoacoustic modes can be modified by the time evolution of an impulsively generated signal. An obvious source of such an impulsive disturbance is a flare (providing either a single or multiple source of disturbances). These fast magnetoacoustic waves are trapped in regions (e.g. coronal loop) with a high density (i.e. with a low Alfvén speed). These regions are acting as waveguides. The impulsively generated (propagating) wave in a density coronal waveguide exhibits several phases: (1) periodic phase (long-period spectral components arrive as the first at the observation point), (2) quasi-periodic phase (as both long and short-period spectral components arrive and interact), and finally (3) decay phase (as the signal passes). The quasi-periodic phase is generally much stronger in amplitude and shorter in 'periodicity' than the earlier periodic phase.

The numerical simulation of characteristic time (wavelet) signatures of impulsively generated fast magnetoacoustic wave trains propagating along a coronal loop with different ratios of the density contrast has been studied by Nakariakov et al. (2004). It was found that the dispersive evolution of fast wave trains leads to the appearance of characteristic tadpole wavelet signature where a narrow-spectrum tail precedes a broadband head. Such tadpole signatures were observed in solar eclipse data (Katsiyannis et al., 2003; Williams et al., 2001). Now, for

* Corresponding author. Tel.: +420 323 620155; fax: +420 323 620210.
E-mail addresses: hana@asu.cas.cz (H. Mészárosová), sawant@das.inpe.br (H.S. Sawant), cecattojr@gmail.br (J.R. Cecatto), choc@astro.sk (J. Rybák), karlicky@asu.cas.cz (M. Karlický), guga@univap.br (F.C.R. Fernandes), con@das.inpe.br (M.C. de Andrade), jiricka@asu.cas.cz (K. Jiřička).

0273-1177/$36.00 © 2009 COSPAR. Published by Elsevier Ltd. All rights reserved.
doi:10.1016/j.asr.2009.01.032

the first time, these tadpole wavelet signatures of impulsively generated fast magnetoacoustic wave trains observed in decimetric type IV radio event are presented.

2. Observation and results

The June 6, 2000 flare (classified as X2.3, GOES X-ray maximum at 15:25 UT) was observed during 14:58–17:00 UT in the active region NOAA AR 9026. In H_α the flare has the importance 2B. We have observed a 22 min long (15:40:05–16:02:00 UT) decimetric type IV radio event during the decay phase of this flare recorded simultaneously by the Brazilian Solar Spectroscope (BSS, frequency range 1200–1700 MHz, time and frequency resolution is 50 ms and 5 MHz, respectively) and by the Ondřejov radiospectrograph (frequency range 2000–4500 MHz, time and frequency resolution is 100 ms and 10 MHz, respectively). The radio spectra for the whole time interval are shown in Fig. 1. The high time and frequency resolutions of both instruments enable us to investigate the spectra in detail. Time series of these spectra have been analyzed in their power and global wavelet spectra at individual frequencies in the range 1200–4500 MHz.

For the analysis, we have divided the interval under study (15:40:05–16:02:00 UT) into four subintervals A–D (Table 1) and we have recognized tadpole wavelet signatures in all these subintervals. An example of the characteristic tadpole pattern (time subinterval C) is shown in Fig. 2. The top panel shows the time series at the frequency 1395 MHz and the middle panel exhibits the corresponding wavelet power spectrum with tadpole pattern as the signature of a coronal fast wave train. The lighter area indicates greater power in the wavelet power spectrum and the hatched region belongs to the cone of influence (COI) where edge effects become important due to dealing with finite-length time series. The solid contour shows the 95% confidence level. In the analysis of each of time series only these contoured regions which exist outside the COI have been considered as valid. The long-period spectral component (tadpole tail) has characteristic period $P = 63.8$ s. The range of periods at the point of the maximal extension of the tadpole head is 39.5–70.1 s. The bottom panel shows the global wavelet spectrum with the characteristic period $P = 63.8$ s above the 95% global significance level (horizontal line). Some examples of tadpoles at different frequencies are presented in Figs. 3 and 4.

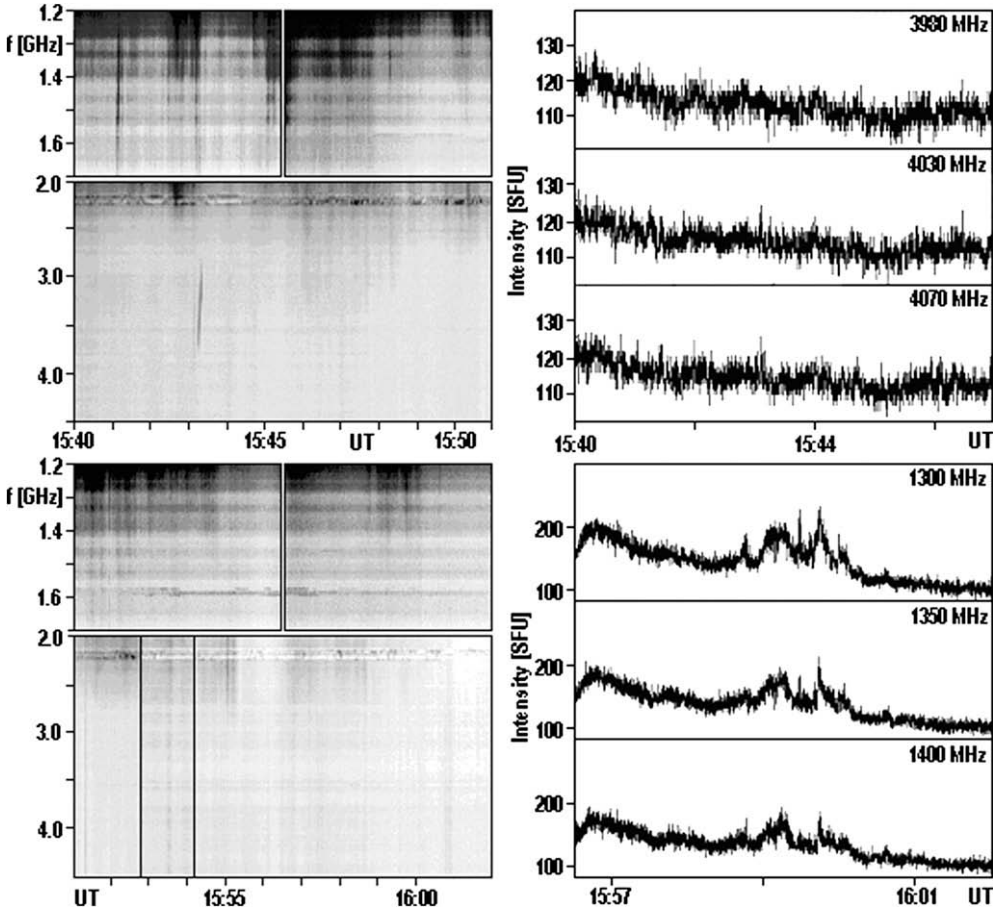

Fig. 1. Left panels: 22 min long decimetric type IV radio spectrum (the highest intensity in black) observed during the decay phase of the June 6, 2000 flare recorded simultaneously by the BSS (1200–1700 MHz) and by the Ondřejov radiospectrograph (2000–4500 MHz). Right panels: characteristic flux time series at six selected frequencies.

Table 1
Time subintervals of broadband pulsations observed during the decay phase of the June 6, 2000 flare in the frequency range 1200–4500 MHz.

Time subinterval	Start (UT)	End (UT)
A	15:40:05	15:45:33
B	15:45:34	15:51:02
C	15:51:03	15:56:31
D	15:56:32	16:02:00

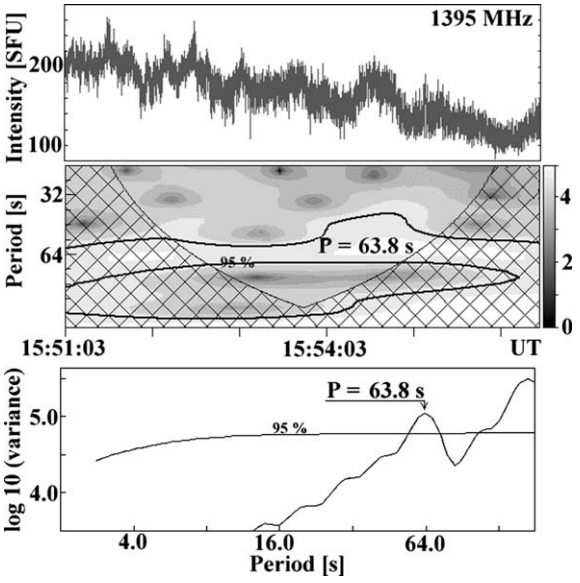

Fig. 2. Example of a tadpole wavelet pattern of a coronal fast wave train. Top panel: time series at the frequency 1395 MHz. Middle panel: corresponding wavelet power spectrum with a tadpole signature. The lighter area indicates a greater power in the wavelet power spectrum and the hatched region belongs to the cone of influence (COI). The solid contour shows the 95% confidence level. The range of powers (grey scale) is presented on right side of the spectrum. The long-period spectral component (tadpole tail) has characteristic period $P = 63.8$ s. Bottom panel: global wavelet spectrum with the characteristic period $P = 63.8$ s above the 95% global significance level (horizontal line).

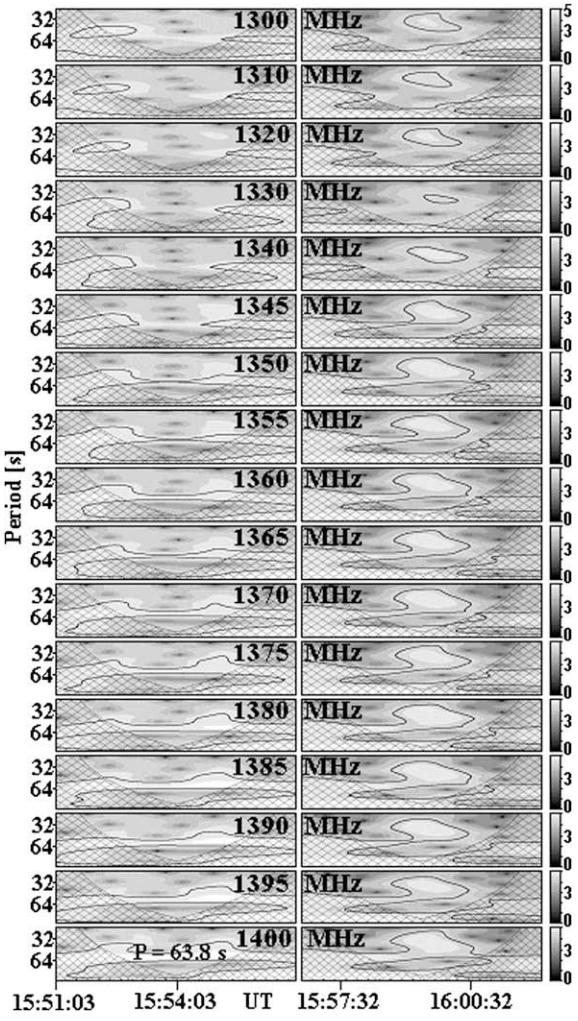

Fig. 3. Tadpole wavelet signatures of coronal fast wave trains and their changes at individual frequencies in the range 1300–1400 MHz (time subintervals C and D). The lighter area indicates a greater power in the wavelet power spectrum and the hatched region belongs to the cone of influence (COI). The solid contour shows the 95% confidence level. The ranges of powers (grey scales) are presented on right side of the spectra (common for spectra in both columns). The long-period spectral components (tadpole tails) of all wave trains have characteristic period $P = 63.8$ s.

Series of two tadpoles (time subintervals C and D) between frequencies 1300 and 1400 MHz can be seen in Fig. 3. The long-period spectral components (tadpole tails) of these wave trains with the characteristic period $P = 63.8$ s propagate faster than the medium and short-period ones. This characteristic period P has on average 2.3 and 1.2 wave oscillations for the tadpoles in left and right column in Fig. 3, respectively. When the duration of long-period spectral component was calculated, any portion within the COI was discarded. The average range of periods in the place of the maximal extension of the tadpole head is 36.9–70.9 and 26.0–65.5 s for tadpoles in the left and right column in Fig. 3, respectively. Some basic tadpole parameters (time subinterval C, Fig. 3) are shown in Table 2 and they are very similar at different frequencies.

Tadpoles occurring between frequencies 3980 and 4070 MHz during time subinterval A are present in Fig. 4. The long-period spectral components of these wave trains have the characteristic period $P = 54.5$ s with 4.5 wave oscillations on average. The average range of periods in the place of the maximal extension of the tadpole head is 26.7–63.1 s. These basic tadpole parameters are shown in Table 3 and they differ at individual frequencies more than in the previous case (Table 2).

There are some differences between individual wave trains (tadpoles) and their behavior at higher frequencies and at lower frequencies. Furthermore, the tadpoles at the same frequency but in different time subinterval (Table 1) have some common as well as different properties.

The two tadpole series in Fig. 3 (time subintervals C and D) occur in the same frequency range 1300–1400 MHz with the same characteristic period $P = 63.8$ s (long-period spectral component) but with the different wave train duration: average 2.3 wave oscillations for the earlier wave train

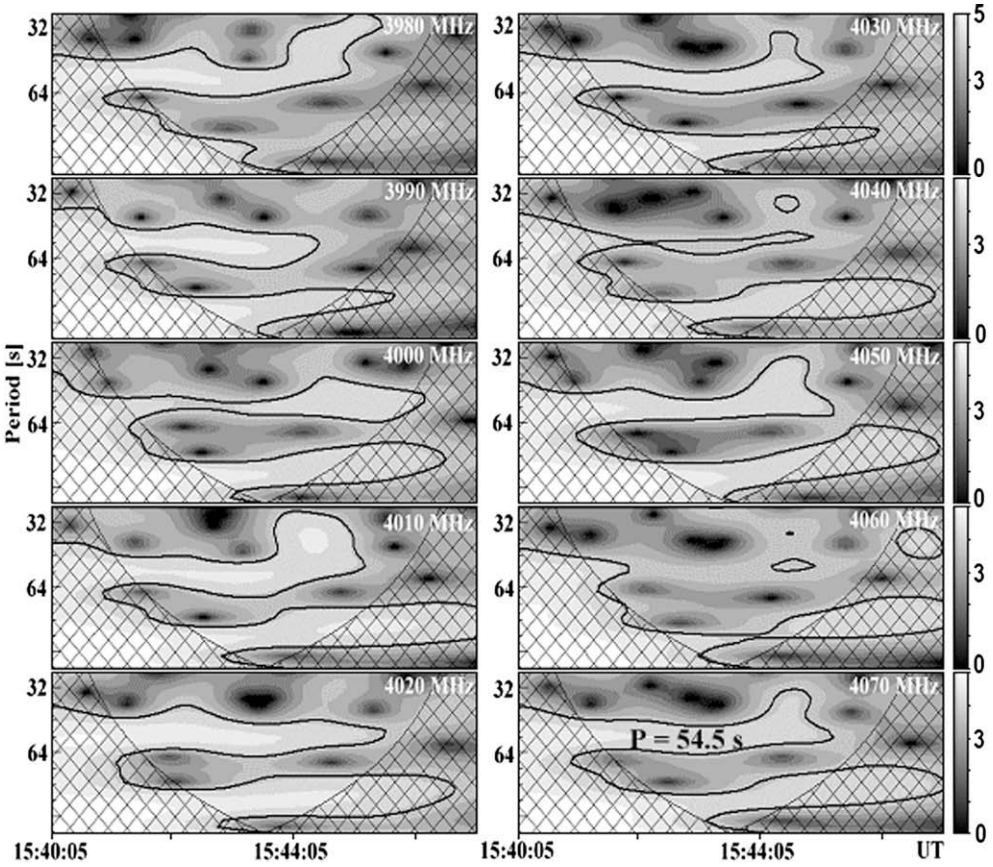

Fig. 4. Tadpole wavelet signatures of coronal fast wave trains and their changes at individual frequencies in the range 3980–4070 MHz (time subinterval A). The lighter area indicates a greater power in the wavelet power spectrum and the hatched region belongs to the cone of influence (COI). The solid contour shows the 95% confidence level. The ranges of powers (grey scales) are presented on right side of the spectra (common for spectra in both columns). The long-period spectral components (tadpole tails) of all wave trains have characteristic period $P = 54.5$ s.

Table 2
Basic tadpole parameters for the time subinterval C (left panels in Fig. 3). All wave trains have characteristic period $P = 63.8$ s (Duration = duration of the tadpole, Oscillations = number of wave oscillations of the period P, Range of periods = range of periods at the point of the maximal extension of the tadpole head).

Frequency (MHz)	Duration (s)	Oscillations	Range of periods (s)
1350	150.6	2.4	48.9–69.3
1355	150.0	2.3	52.9–68.5
1360	150.0	2.3	50.0–70.1
1365	150.0	2.3	49.5–68.5
1370	149.4	2.3	44.7–69.3
1375	151.3	2.4	37.7–69.3
1380	148.7	2.3	37.7–70.9
1385	150.0	2.3	40.8–70.9
1390	151.4	2.4	43.2–70.1
1395	149.4	2.3	39.5–70.1
1400	151.8	2.4	36.9–70.9

Table 3
Basic tadpole parameters for the time subinterval A (see Fig. 4). All wave trains have characteristic period $P = 54.5$ s (Duration = duration of the tadpole, Oscillations = number of wave oscillations of the period P, Range of periods = range of periods at the point of the maximal extension of the tadpole head).

Frequency (MHz)	Duration (s)	Oscillations	Range of periods (s)
3980	205.0	3.8	26.7–59.1
3990	187.5	3.4	
4000	281.3	5.2	38.8–63.1
4010	217.6	3.4	27.9–61.8
4020	250.5	4.6	
4030	206.7	3.8	32.9–62.4
4040	188.2	3.4	47.9–54.4
4050	235.8	4.3	31.2–59.1
4060			
4070	234.4	4.3	32.2–58.4

(time subinterval C) and 1.2 wave oscillations for the later one (time subinterval D). Moreover, the appearance of both wave trains is different. In the case of the earlier wave train (left column of panels in Fig. 3) we can see a full tadpole structure (tail + head) to the frequency 1370 MHz. Then, in direction to the lower frequencies, the head is fading and from the frequency 1345 MHz the whole tadpole is decayed. In the case of the later wave trains (right column of panels in Fig. 3) we can see a full tadpole structure to the frequency 1340 MHz where the tadpole is decayed and at lower frequencies we can see only a rest of the tadpole head. The tadpole patterns of the individual wave trains (in the same time interval) at lower frequencies (Fig. 3) are very similar to each other i.e. their changes from frequency to frequency are slow.

Different tadpole behavior can be seen at higher frequencies (3980–4070 MHz) in Fig. 4 (time subinterval A). There is a set of different tadpoles but with the same characteristic period $P = 54.5$ s (long-period spectral components) and with a similar duration (on average 4.5 wave oscillations). The process of tadpole appearance and fading (see tadpoles at frequencies 4030–4070) is significantly more rapid and repeating. Individual tadpoles have different heads (set of middle and short-period spectral components) and in some cases the head is absent (see tadpoles at frequencies 3990 and 4020 MHz). Sometimes, the whole tadpole is fully absent (for example at 4061 MHz).

3. Conclusions

We have investigated the 22 min long decimetric type IV of radio event during the decay phase of the June 6, 2000 flare observed simultaneously by the BSS and the Ondřejov radiospectrograph (1200–4500 MHz). For the first time, the tadpole structures of dm-radio event are evident in their wavelet power spectra in the whole time interval and at all frequencies. We have distinguished the tadpole wavelet signatures in our observational data and it allows us to identify the corresponding waves as fast magnetoacoustic wave trains. These waves are probably trapped in a waveguide (e.g. loop) and formed by an impulsive source (e.g. flare or reconnection process). We present two examples of tadpoles (Figs. 3 and 4) with different behavior but similar characteristic period P (long-period spectral component of all wave trains) of about 60 s.

The tadpoles in Fig. 3 show relatively slow changes of the same tadpole at different frequencies. It may reflect that at the lower frequencies the plasma density is more smooth (no abrupt changes in density). These tadpoles have short duration of long-period spectral component (low number of wave oscillations of the characteristic period) i.e. wave damping is strong here. Furthermore, these tadpoles can decay at the lowest frequencies under study (Fig. 3). This may represent less density contrast (density ratio between external and internal plasma density of a loop) which causes that such a segment of a loop is a worse waveguide.

Tadpoles at higher frequencies (Fig. 4) have longer duration of long-period spectral component (higher number of wave oscillations of their characteristic period P). On the other hand, the individual tadpoles show very rapid changes of the same tadpole at different frequencies. Thus, individual tadpoles are different (mainly with respect to their heads, i.e. their middle and short-period spectral components). Sometimes, we can observe only the long-period spectral component (tail) of the wave train that arrives as the first at the observable point. This can represent a higher diversity in plasma density of a loop (more rapid changes of plasma density inside such a loop segment). The wave damping is strong also in this case.

We have distinguished two groups of individual tadpoles with different properties: the first tadpole group was detected in the frequency range 1200–1600 MHz (time subintervals C and D, Fig. 3) and the second group in the frequency range 3800–4500 MHz (time subinterval A, Fig. 4). Thus, each group can belong to a different radio emission source. If one emission source is dominant we can detect individual tadpoles with similar properties. On the other hand, the wavelet power spectra are more complex (chaotic) in the frequency range 1600–3800 MHz (i.e. we cannot see individual tadpoles). It can happen when the time series in this frequency range are influenced for example, by more than one emission source.

The tadpoles can provide an evidence for MHD waves in the corona. They may provide the basics for determination of the transverse structure, density distribution and other properties of the waveguide (coronal loop).

Acknowledgements

H.M. acknowledges the FAPESP support for the project 2006/50039-7. H.M. and M.K. acknowledge the support from the Grant IAA300030701 of the Academy of Sciences of the Czech Republic. F.C.R.F. thanks CNPq for scholarship (proc. 310005/2005-1). J.R.C. acknowledges the CNPq support for project 475723/2004-0. J.R. acknowledges the support of the grant agency VEGA 02/6195/26. The wavelet analysis was performed using the software based on tools provided by C. Torrence and G. Compo at http://paos.colorado.edu/research/wavelets/.

References

Katsiyannis, A.C., Williams, D.R., McAteer, R.T.J., et al. Eclipse observations of high-frequency oscillations in active region coronal loops. A&A 406, 709–714, 2003.

Nakariakov, V.M., Arber, T.D., Ault, C.E., et al. Time signatures of impulsively generated coronal fast wave trains. Mon. Not. Roy. Astron. Soc. 349, 705–709, 2004.

Roberts, B., Edwin, P.M., Benz, A.O. Fast pulsations in the solar corona. Nature 305, 688–690, 1983.

Roberts, B., Edwin, P.M., Benz, A.O. On coronal oscillations. Atrophys. J. 279, 857–865, 1984.

Williams, D.R., Phillips, K.J.H., Rudawy, P., et al. High-frequency oscillations in a solar active region coronal loop. Mon. Not. Roy. Astron. Soc. 326, 428–436, 2001.